Springer

Journal of Mechanical Science and Technology 22 (2008) 2107~2121

Journal of Mechanical Science and Technology

www.springerlink.com/content/1738-494x
DOI 10.1007/s12206-008-0613-4

Diagnosis and control of machine induced noise and vibration in steel construction †

Wei-Yu Lu* and Wei-Hui Wang

Sound and Vibration Research center Department of Systems Engineering and Naval Architecture
National Taiwan Ocean University, Pei-Ning Rd.#2, Keelung, Taiwan

(Manuscript Received July 10, 2007; Revised May 3, 2008; Accepted June 17, 2008)

Abstract

Most high-rise buildings constructed of steel or steel reinforced concrete have to install various vital equipments. Among these equipments machinery noise is especially annoying for accommodation close to them. In attempting to control the machine-induced structure-borne noise and vibration, the methodology by employing mobility functions to identify the dominant frequency band of vibrational power flow transmission and to assess the isolation effectiveness of isolators is established. The proposed method of diagnosis procedure is applied to the structure-borne vibration power flow transmission for a steel construction parking tower. After proper check and replacement of the isolators of the power unit platform of the mechanical parking tower, the improvement results in a substantial structure-borne noise reduction of 16 dB(NC). The unique parts of the paper include the establishment of the relation of mobility functions with respect to four-pole parameters for a coupled machine/mount/foundation system. Also expressions to represent the vibrational input power, the output power and the transmitted power in relation to mobility functions are clarified.

Keywords: Structure-borne noise; Vibrational power flow; Resilient mount; Multi-path sound transfer; Diagnosis and identification

1. Introduction

In order to substantialize the development of green buildings with the concept of environmental protection, such as energy saving, resources reduction and recycling, light weight steel structures are encouraged to construct in replacing the traditional reinforced concrete (RC) or wooden structures. Meanwhile, owing to the 1999 Chi-Chi earthquake in Taiwan and the emerged trend of green building requirement, SRC(steel reinforced concrete) and SC (steel construction) buildings are widely favorite to adopt by architects in recent years, for the purpose of promoting earthquake withstanding capability and material weight saving and recycling.

As a number of building service equipments, such as pumps, ventilators and air conditioners, emergency generator, cooling tower and mechanical parking tower etc., are installed in SC buildings, inevitably, the machine induced structure-borne noise and vibration can be a serious problem for accommodation close to the machine equipments. In recent years, Wang and Lu [1, 2] have coped with the diagnosis and improvement works regarding to the structure-borne noise generated by condensers and compressors for a high capacity air-conditioner, cooling tower, mechanical parking tower, transformer, pipe flow etc., in various SC buildings. From these experiences and the increasing complaints to the machine generated lower frequency noise, it can illustrate the emerging seriousness of structure-borne noise and vibration existing in SC buildings.

In surveying of a number of bibliographies, it can be seen that the structure-borne sound power is predominantly transmitted to a sound carrying structure from a source via a number of contact points with a

† This paper was recommended for publication in revised form by Associate Editor Seong-Wook Hong

*Corresponding author. Tel.: +886 932 023 043, Fax.: +886 2 2547 4975
E-mail address: luweiyu6050@yahoo.com.tw

machine. In turn, the noise and vibrations are propagated in the structure to cause undesired radiated noise. In principle, this can be avoided by countermeasures at source, in transmission, during propagation or at radiation. It is, of course, preferable to cope with the problems at the generation sites and thereby avoid more comprehensive and expensive measures later in the chain. To this end, the resilient mounts are utilized as an effective countermeasure to reduce noise and vibration power transmitted from the source to sound receiver.

In reviewing noise transmission paths, Lu and Wang noted that from a machine to other areas of a SC building the transmission characteristic is relative longer in wave length and faster in wave speed than that transmitted in a RC buildings [1]. Noise propagation in SC structures as well as the choice of appropriate control measures is intimately related. Since the machine induced vibration force and velocity may not be in phase, and sometimes, a large response in a structure does not always lead to a higher level radiated noise, hence a more appropriate power flow method which was ever applied in Ref. [3,4,5,6], is adopted in the study. The effectiveness of isolators can be evaluated by the power transmitted to the structure. This single quantity includes both the vibration parameters of force and velocity. An important reason for using the concept of power is that it provides a means of comparing the effects of both translational and rotational excitations. Minimizing the power transmitted through an isolator is also consistent with the first step in any vibration control exercise, i.e., to deal with the problem at the source.

The vibrational power fed into a structure for a multipoint mounting system can be calculated by utilizing the concept of effective mobility of the source/mount/ receiver system and the source characterization as a force or a velocity. This kind of characterization has ever considered in [7, 8]. To achieve a successful design and an appropriate selection of the mount, sensitivity analyses of the mobility function value with respect to the dynamic properties should be undertaken.

2. Mobility theory and power flow transmission

The mobility of a structure is the ratio between velocity and force for simple harmonic vibration in the range of linear behavior. The term point mobility is used where velocity and force are at same position and in the same direction. While the term transfer mobility is used when velocity and force are at different positions and/or different direction.

2.1 Mobility of multipole coupling system

Structure-borne noise transmission caused by mechanical coupling between machine (source) and seating structure via a resilient mount can be represented as shown in Fig. 1. By assuming that it can be simplified to a 1-direction coupling then it may be modeled as an isolator suspension system. Assumed that the resilient mount is input and output with instantaneous force F_1 and F_2 respectively, and results in corresponding instantaneous velocities V_1 and V_2. The dynamic behavior of this coupled system can be expressed in terms of frequency response characteristics.

Put the ratio $\frac{V_1}{F_1} = M_{11}$ to be the point mobility at 1 and $\frac{V_2}{F_1} = M_{21}$ to be the transfer mobility at 2 induced by force acting at 1. For linear system the transfer mobilities M_{21} and M_{21} are reciprocal, i.e. $M_{21} = M_{12}$. The velocity vector $\begin{Bmatrix} V_1 \\ V_2 \end{Bmatrix}$ is related to the force vector $\begin{Bmatrix} F_1 \\ F_2 \end{Bmatrix}$ by the full mobility matrix, i.e.

$$\begin{Bmatrix} V_1 \\ V_2 \end{Bmatrix} = \begin{bmatrix} M_{11} & M_{12} \\ M_{21} & M_{22} \end{bmatrix} \begin{Bmatrix} F_1 \\ F_2 \end{Bmatrix} \tag{1}$$

Eq. (1) represents the dynamic behavior of an individual resilient mount subsystem. In reality, a mechanical-structure system has a number of N resilient mounts arranged in parallel connection, therefore the mobility coefficient can be written as:

$$M_{ij}(\omega) = \sum_{r=1}^{N} \frac{j\omega A_{ijr}}{\left(\omega_r^2 - \omega^2\right) + j\eta_r\omega_r^2} \tag{2}$$

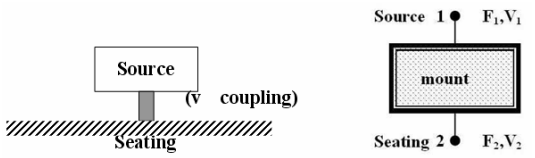

Fig. 1. Machine-mount-seating structure coupling system.

where $A_{ijr} = \Phi_{ir}\Phi_{jr}$ is the modal constant; $[\Phi]$ is the mass normalized modal matrix; ω_r is the undamped natural frequency of the rth mode; ω is the exciting frequency; η_r is the structural damping loss factor of the rth mode; $j = \sqrt{-1}$。

2.2 Vibrational power input to a receiving structure from machine

The instantaneous vibration power input (P_{inst}) to a structure is defined as the product of the excitation force (F) and the associated velocity (V). For a harmonic excitation $|\mathrm{F}| \sin \omega t$ applying at a point on a structure of mobility, $M = |M| e^{j\phi}$, it causes a velocity $|V| \sin(\omega t + \phi)$ at that point, where ϕ is the phase angle between the driving excitation force and the associated velocity. The instantaneous vibrational power input will be:

$$(P_{inst}) = F V^* = |F| \, |V| \sin\omega t \, \sin(\omega t + \phi) \tag{3}$$

where V^* is the conjugate of complex velocity V.

In general, it is of greater interest to know the time averaged power input (P). It is calculated by integrating Eq. (3) over one period of vibration to yield:

$$\begin{aligned}(P) &= \frac{1}{T}\int_0^T |F| \, |V| \, \sin\omega t \, \sin(\omega t + \phi)\, dt \\ &= \frac{1}{2}|F||V|\cos\phi\end{aligned} \tag{4}$$

The averaged power input is related to the phase angle ϕ. If $\phi = \frac{\pi}{2}$ i.e., undamped, then the averaged power (P)=0.

At any point on a structure, the velocity and force are related via frequency response mobility (or impedance) functions, so that Eq. (4) may be rewritten in the following forms:

$$(P) = \frac{1}{2}|F|^2 \mathrm{Re}[M] \tag{5}$$

or

$$(P) = \frac{1}{2}|V|^2 \mathrm{Re}[Z] \tag{6}$$

where Re[M] and Re[Z] are the real part of the point mobility function and the point impedance function at the excitation site, respectively. The choice of which equation to apply in a practical situation is controlled by the nature of the vibration source and the ability to measure either the force or velocity. In many cases, Eq. (6) can be applied if a machine is unaffected by the method of attachment, such that it behaves on site as if it were freely suspended. For a machine mounted on an isolation system, this condition is usually fulfilled velocity source.

The above equations are applicable only to a harmonically varying point force. In general, machinery is supported at a number of sites and each site will have some contact area over which both direct forces and moments may be transmitted. This will lead to a very complicated set of inter-related expressions for the total input power. Suppose that there are N coordinates involved in the coupling of the machine to the sub-structure, then it will be necessary to define an N×N matrix of mobility functions. Eqs. (5) and (6) are rewritten in matrix form as:

$$(P) = \frac{1}{2}\{F\}^T \mathrm{Re}[M]\{F\} \tag{7}$$

or

$$(P) = \frac{1}{2}\{V\}^T \mathrm{Re}[Z]\{V\} \tag{8}$$

Prediction, or measurement, of (P) value via these full matrix relationships can be extremely difficult. This is particularly true in situations where moment excitations represent a major source of the resultant vibrational power.

From Eqs. (7) and (8), it is clear that the power injected into a structure by the machine is dictated by the excitation force or velocity exerted by a machine and the mobility or impedance characteristics of the supporting structure. The characterization of a machine as a " velocity source" will now be considered .

There are many techniques available for modelling engineering structures in order to predict the mobility frequency response functions. These include finite element analysis, experimental modal analysis and analytical techniques based upon the use of infinite structures. Finite element analysis and experimental modal analysis are limited in their application to frequencies whose behavior can be described as "moda". For a finite element model, this implies that the use of many degrees of freedom may lead to difficulties and

can be a serious concern. Pinnington has shown that relatively simple models of "patches" around mounting sites can be used to predict the higher frequency performance of a seating structure [9]. The introduction of realistic damping (which is essential if one is seeking to estimate the mathematically real component of the mobility function) into the preliminary modeling phase of a finite element idealization also poses a problem in many instances. However, it is possible to introduce a form of modal damping, extracted from experimental observations, into the calculations of frequency domain data based upon a finite element model.

In practical measurements by utilizing a FFT analyser, the power can be found by using the force spectrum density function G_{ff} , or the vibration velocity spectrum density function G_{vv}, or the cross power spectrum density function G_{fv} , which can be expressed as:

$$P(\omega) = G_{ff}\ \mathrm{Re}[M] = \mathrm{Re}[G_{fv}] = G_{vv}\ \mathrm{Re}[Z] \tag{9}$$

The driving point impedance matrix, the receiving point impedance matrix and the transfer impedance matrix for well-installed system can be obtained as:

$$[Z_{input}] = [Z_{11}] = \frac{[M_{22}]}{[M_{11}][M_{22}] - [M_{12}][M_{21}]} \tag{10a}$$

$$[Z_{output}] = [Z_{22}] = \frac{[M_{11}]}{[M_{11}][M_{22}] - [M_{12}][M_{21}]} \tag{10b}$$

$$[Z_{transmit}] = [Z_{21}] = [Z_{12}] = \frac{-[M_{12}]}{[M_{11}][M_{22}] - [M_{12}][M_{21}]} \tag{10c}$$

Substituing $[Z_{input}]$, $[Z_{output}]$ and $[Z_{transmit}]$ into Eq. (9), the input power, output power and transmitted power can be calculated respectively, i.e.

$$(P_{input}) = G_{V_A V_A}\ \mathrm{Re}[Z_{input}] \tag{11a}$$

$$(P_{output}) = G_{V_B V_B}\ \mathrm{Re}[Z_{output}] \tag{11b}$$

$$(P_{transmit}) = G_{V_A V_A}\ \mathrm{Re}[Z_{transmit}] \tag{11c}$$

Thus the general methodology for obtaining the power fed into a receiving structure from the excitation sources of a machine via the contact points is derived.

2.3 Logic of structure-borne sound reduction

The low noise design for a simple machine installed in a structure is schematically shown in Fig. 2. The primary noise generating mechanism is the machine that injects vibrations into the structure via the mounts and foundations. These vibrations will be transmitted throughout the structure and eventually radiate sound to the surroundings.

To simulate the vibration reduction behaviour of the resilient mounts of a machine, a model can be established by utilizing simple input/output transfer mechanisms, which may be represented in terms of mobility functions. Fig. 2(b) and 2(c) show the analysis models which can be used to represent the structure-borne sound transfer between the primary source and the radiating surface. For a uni-directional simple harmonic excitation force F_1 , the machine vibrates with a simple harmonic velocity V_1 at the driving point. Structural waves propagate from the excitation point to the adjacent floors, where bending waves generate a velocity field V_2 (x,y). This vibration field radiates a sound pressure field p (x,y,z).

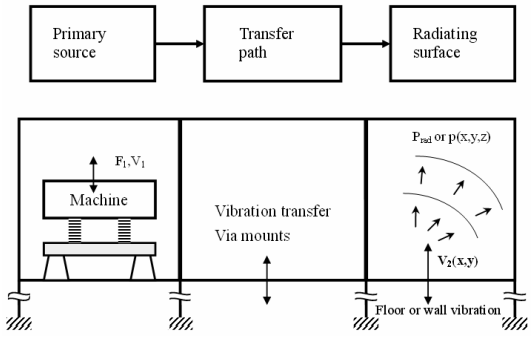

(a) Structure-borne noise transfer

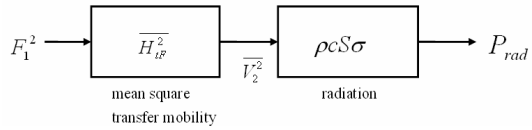

(b) Energetic model "force excitation"

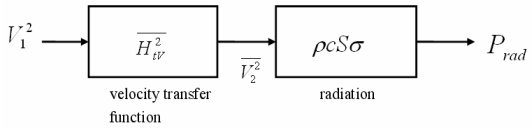

(c) Energetic model "velocity excitation"

Fig. 2. Schematic of machine induced structure-borne noise analysis for low noise design.

The linear equations which relate the radiated sound pressure with the force and the velocity at the driving point are [10]:

$$p(x,y,z,f)=H_{tF}F_1(f) \quad (12)$$

$$p(x,y,z,f)=H_{tV}V_1(f) \quad (13)$$

where H_{tF} and H_{tV} are so-called frequency response functions, describing the sound transfer for force and velocity excitation respectively. Basically, these frequency response functions have a complex value at each frequency, indicating the magnitude and the phase of the vibration.

The force and velocity at the diving point are related as

$$M_{11}=\frac{V_1}{F_1} \quad (14)$$

Where M_{11} is called driving point mobility. It is a measure of the vibration velocity for a given force F_1.

In many practical situations instead of linear equations, equations in terms of mean square quantities or so-called "energetic" quantities are used. In principle, these formulations are exact, if derived directly from Eqs. (12) and (13). However, for practical purposes, approximations of transfer functions are used. Those functions relate e.g. 1/3-octave band levels of F_1^2 and V_1^2 with the radiated sound power P_{rad} [10]. In the scheme of Figs. 2(b) and 2(c), the " energetic " models are presented. The transmission chain is divided into two blocks. The first block represents the structure and gives the ratio between the spatially averaged mean square velocity $\overline{V_2^2}$ of the floor surface and F_1^2 or V_1^2:

$$M_{21}^2=\frac{\overline{V_2^2}}{F_1^2} \quad , \quad H_{tV}^2=\frac{\overline{V_2^2}}{V_1^2} \quad (15)$$

The function M_{21}^2 is called the mean square transfer mobility and the function H_{tV}^2 is called the velocity transfer function.

The second block represents the sound radiation and gives the ratio between the radiated sound power P_{rad} and $\overline{V_2^2}$:

$$\frac{P_{rad}}{\overline{V_2^2}}=\rho cS\sigma \quad (16)$$

The right side of Eq. (16) contains the characteristic impedance ρc of the surrounding air, the area S of the radiating surface, and the radiation efficiency σ. σ is a measure of the efficiency with which a structure converts vibrations into sound.

The factors which determine the sound transfer is influenced by design as seen in Fig. 2 and from the following equations:

$$\frac{P_{rad}}{F_1^2}=(M_{21}^2S\sigma)\rho c=(M_{11}^2H_{tV}^2S\sigma)\rho c \quad (17)$$

$$\frac{P_{rad}}{V_1^2}=(H_{tV}^2S\sigma)\rho c \quad (18)$$

If the nature of the excitation is such that for different machine design F_1 is unaffected, Eq. (17) implies that sound reduction is obtained by: (a) decrease of driving point mobility; (b) reduction of radiating surface area; (c) decrease of velocity transfer function; (d) decrease of radiation efficiency.

If the nature of the excitation is such that for different engine designs V_1 is unaffected, Eq. (18) implies that sound reduction is obtained by: (a) reduction of radiating surface area; (b) decrease of velocity transfer function; (c) decrease of radiation efficiency.

A design measures to decrease S significantly, have very limited applications. However measures to decrease M_{11} and are H_{tV}^2 are very important and will be adopted extensively in this study.

2.4 Explaination of reduction in transfer mobility by inserting isolator

Suppose the two ends of the subsystems a, b are 1, 2 and 3, 4 respectively, as shown in Fig. 3, where F_i and V_i represent force and velocity. When the subsystems are links together, then $V_3=V_2$ and $F_3=-F_2$. The state vectors at each end can be related by:

$$\begin{Bmatrix} V_1 \\ F_1 \end{Bmatrix}=\begin{bmatrix} \alpha_{11} & \alpha_{12} \\ \alpha_{21} & \alpha_{22} \end{bmatrix}\begin{Bmatrix} V_2 \\ F_2 \end{Bmatrix}$$
$$=\begin{bmatrix} \alpha_{11} & \alpha_{12} \\ \alpha_{21} & \alpha_{22} \end{bmatrix}\begin{bmatrix} \alpha_{33} & \alpha_{34} \\ -\alpha_{43} & -\alpha_{44} \end{bmatrix}\begin{Bmatrix} V_4 \\ F_4 \end{Bmatrix} \quad (19)$$
$$=\begin{bmatrix} \alpha'_{11} & \alpha'_{14} \\ \alpha'_{41} & \alpha'_{44} \end{bmatrix}\begin{Bmatrix} V_4 \\ F_4 \end{Bmatrix}$$

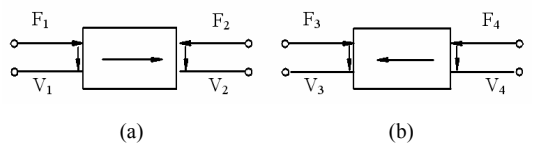

Fig. 3. Mobility of integrated system combined by mobility matrices of the subsystems.

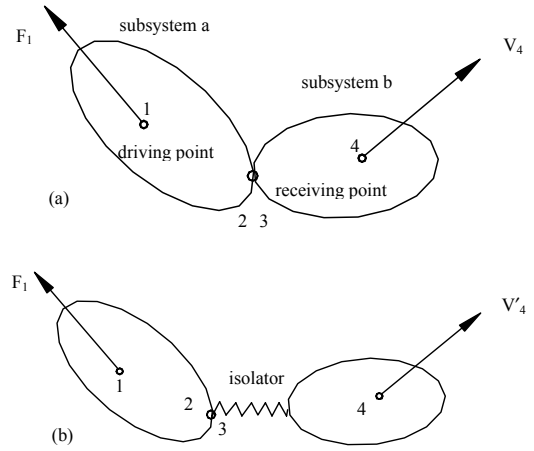

Fig. 4. System before and after installation of isolator.

where α_{ij} and $\alpha_{ij}^{'}$ are the four-pole parameters [11]. It requires that $F_4 = 0$ since 4 is the receiving point and 1 is the driving point. Thus,

$$\frac{1}{\alpha_{41}'} = M_{41} = \frac{V_4}{F_1} \tag{20}$$

From Eqs. (19) and (20)

$$\alpha_{41}' = \alpha_{21}\alpha_{33} - \alpha_{22}\alpha_{43} = \frac{M_{22} + M_{33}}{M_{12}M_{34}}$$

or

$$M_{41} = \frac{M_{12}M_{34}}{M_{22} + M_{33}} \tag{21}$$

Form Eq. (21), it can be seen that the transfer mobility of the combined system M_{41} is not a simple additive combination of the transfer mobilties (M_{12} and M_{34}) of the two subsystems.

The linking point mobilities (M_{22} and M_{33}) of the subsystems play a vital role in determining the total transfer mobility. As an isolator is connected to the input end of the subsystem b, such as in Fig. 4(b) which represents the improved system of Fig. 4(a), the mobility M_{33} would increase significantly. It follows from Eq. (21) that the total transfer mobility M_{41} is reduced. In other words, to reduce the total transfer mobility, it requires the introduction of a larger mobility than the original one. This is the reason of the basic principle for a good structure-borne noise attenuation result that, the structure on both sides of a resilient mount must be properly designed with smaller mobility than that of the mount itself. Simply said, the desired mobility changes for the coupled machine-resilient mount-foundation structure in series system should be "heavy-compliant-heavy" and/or "stiff-compliant-stiff".

3. Screening and identification of transmission behavior for structure- borne sound from a mechanical parking tower in SC building

Owing to the differences of material properties in mass density, Young's modulus and loss factor for SC and RC structure, the structure-borne sound propagation generated by a machine may be different in the stress wavelength, propagation speed and transfer mobility. This can be illustrated by the following comparison analyses.

3.1 Comparisons of mobility and vibration response for SC and RC structures

Consider a 3-bay 5-story SC and RC structures respectively with the same configuration as shown in Fig. 5, but different in column scantlings and material properties. These data are listed in Table 1. When a unit harmonic force is applied vertically at the roof center A, then the transfer mobilities at the center points, B,C,D,E of each floor can be analyzed by the software ANSYS 8.0, which is coded on the basis of finite element method. In the analysis, 240 shell-63 elements and 160 beam-4 elements are used. Fig. 6 shows the comparisons of the transfer mobilities at points B,C,D,E respectively for the SC and RC structure. When a machine operating at point A, whose force spectrum is shown in Fig. 7, the vibration responses at points B,C,D,E of the SC and RC structures are analyzed and the results are compared as shown in Fig. 8. From Fig. 6, it can be seen that the transfer mobility spectra of the SC structure exhibit higher than that of the RC structure in an extensive area of the building and in a broad band of frequency range from 20 to 1 kHz. Also the vibration velocity responses appear the similar phenomenon according to the comparisons of Fig. 8.

Table 1. Material properties and scantling of the SC and RC building.

Material property and scantling / Construction	Young's modulus (N/m^2)	Poisson's ratio	Density (kg/m^3)	Damping ratio ξ	Scantling	
					Column sect. (mm)	Floor thickness (mm)
SC	2×10^{11}	0.3	7800	0.0126	140 x 100 -120 x 80	200
RC	3.25×10^{10}	0.2	2400	0.063	500 x 500	200

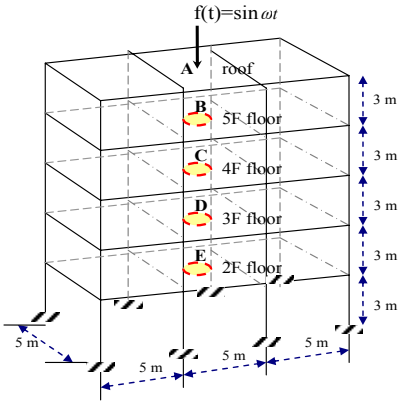

Fig. 5. Configuration of SC and RC structure for mobility comparison.

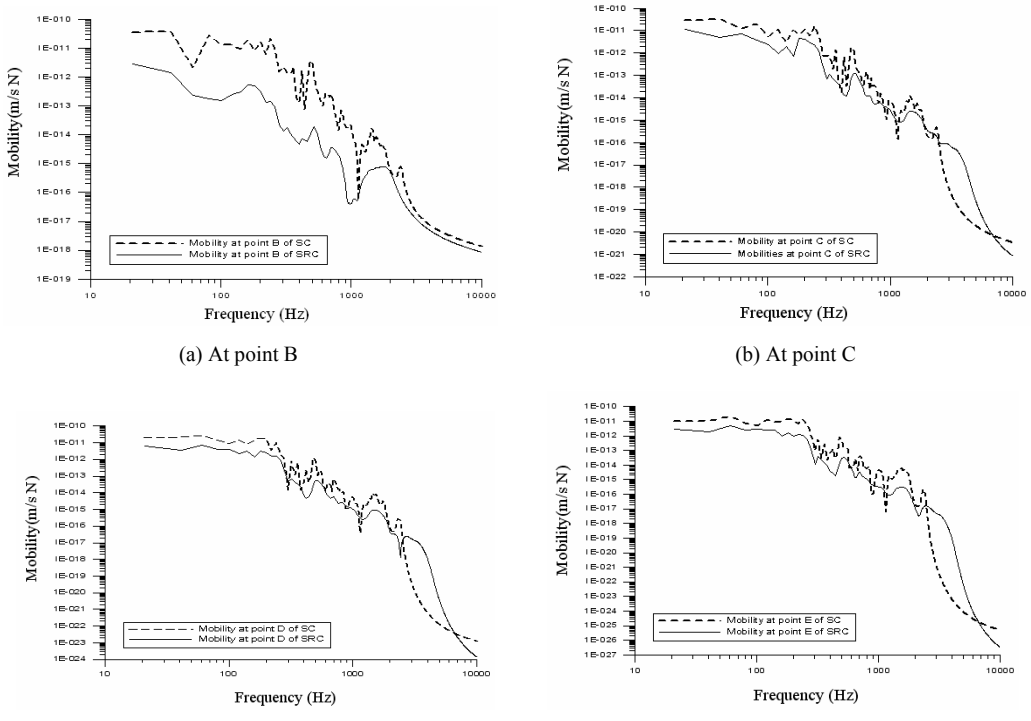

(a) At point B

(b) At point C

(c) At point D

(d) At point E

Fig. 6. Comparison of transfer mobilities of SC and SRC buildings at different locations.

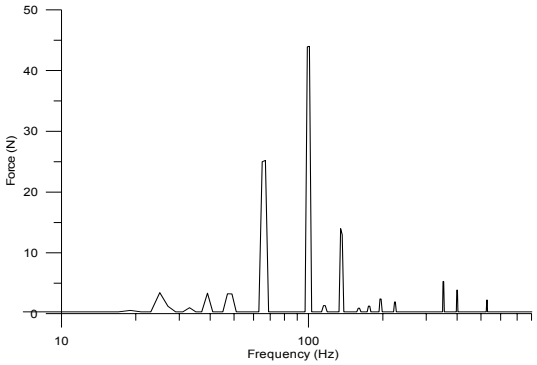

Fig. 7. Force spectrum of a machine applied at point A.

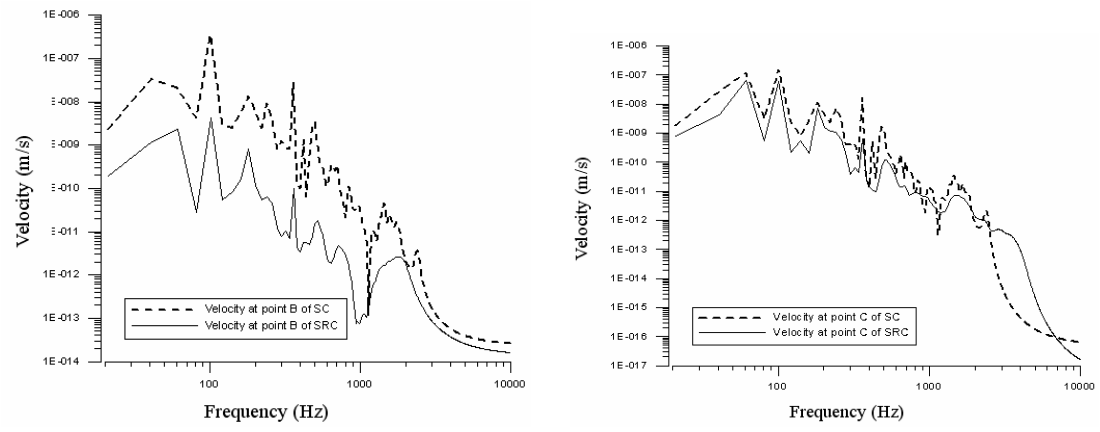

(a) At point B

(b) At point C

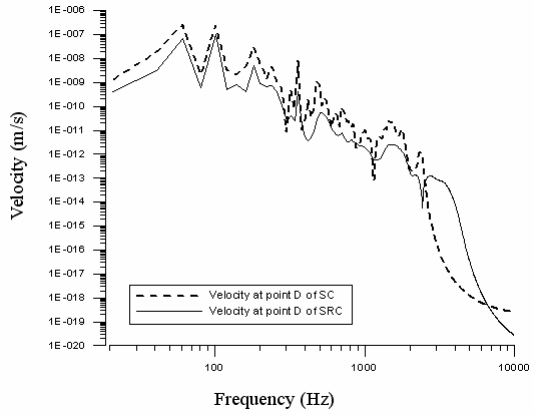

(c) At point D

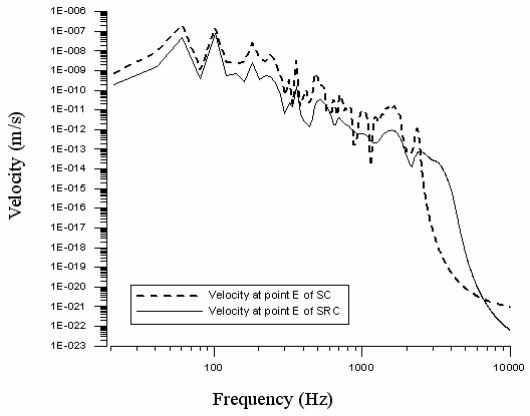

(d) At point E

Fig. 8. Comparison of vibration velocity spectra of SC and SRC buildings at different locations.

3.2 Identification of structure- borne sound transmission from parking tower in SC structure

As an application example, the identification of structure-borne noise transmission from the mechanical parking tower installed in the underground six stories of a high-rise SC building, as shown in Fig. 9, is taken into account. Problem is that when the mechanical power unit operates to drive the parking platform moving up and down, the vibration generated by the running motor, the hoisting winch and cables are transmitted into foundation structure which

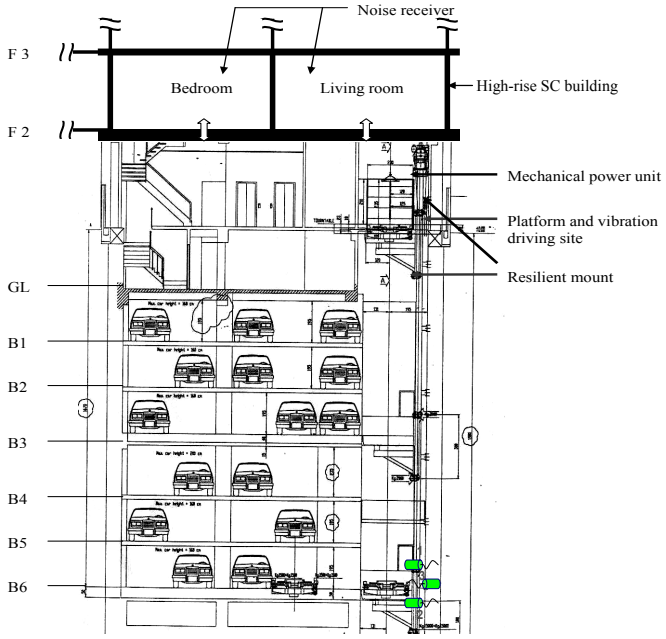

(a) Parking tower arrangement in a SC building

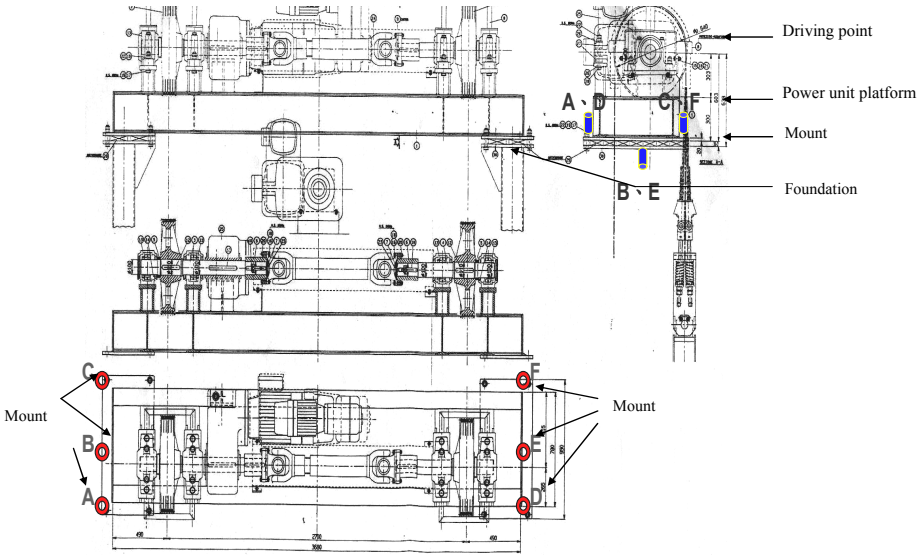

(b) Parking tower arrangement in a SC building

Fig. 9. Parking tower arrangement and mechanical power unit.

is linked to the columns and beam of the SC building by bolts via four rubber mounts A,C D and F. In tern, the vibrations are propagated in the structure to cause undesired radiated noise in the accommodation space upstairs.

What the improvement design concerns is to ascertain the vibration transmission behavior via the original rubber mounts at first. Using the energetic modal and in-site measurements for the transfer mobilities and the vibration spectra along the transmission chain, i.e., from the mechanical power unit via mounts and SC structure elements to the 2nd floor of the building, the power flow through each mount is calculating according to Eq. (8). Fig. 10 are the power spectrum transmitted from source to the under sides of each mount. From which, it is evident that the predominant transmitted power components range in 50 ~ 300 Hz. This coincides with the floor vibration spectrum and sound spectrum measured in the 2nd accommodation space of the SC building, as shown in Figs. 11 and 12.

Aim at raising the isolation effectiveness of the isolators in the frequency range 50 ~ 300 Hz, the original rubber mounts are replaced by spring mounts with the natural frequency of each new mount keeping below 15 Hz. To validate the improvement effectiveness of the new replaced isolators, the isolation levels are measured. Figs. 13 to 18 show the contrast of isolation levels and transmitted vibration acceleration level between the replaced isolators and the original ones.

The spectra of the floor vibration and the noise distribution at the accommodation of the 2nd floor in the SC building, during the operation of the parking tower after the replacement of new selected mounts, are measured and compared with that of the original ones as also shown in Figs. 11 and 12 respectively. To summarize the improvements with respect to the rank of the dominant frequencies, Table 2, 3 show the amount of noise reduction, in dB(A) and dB(NC) respectively and Table 4 lists the vibration attenuation amount in the 2nd floor accommodation. Table 5 shows the values of vibration isolation by new mounts in the dominant frequency band.

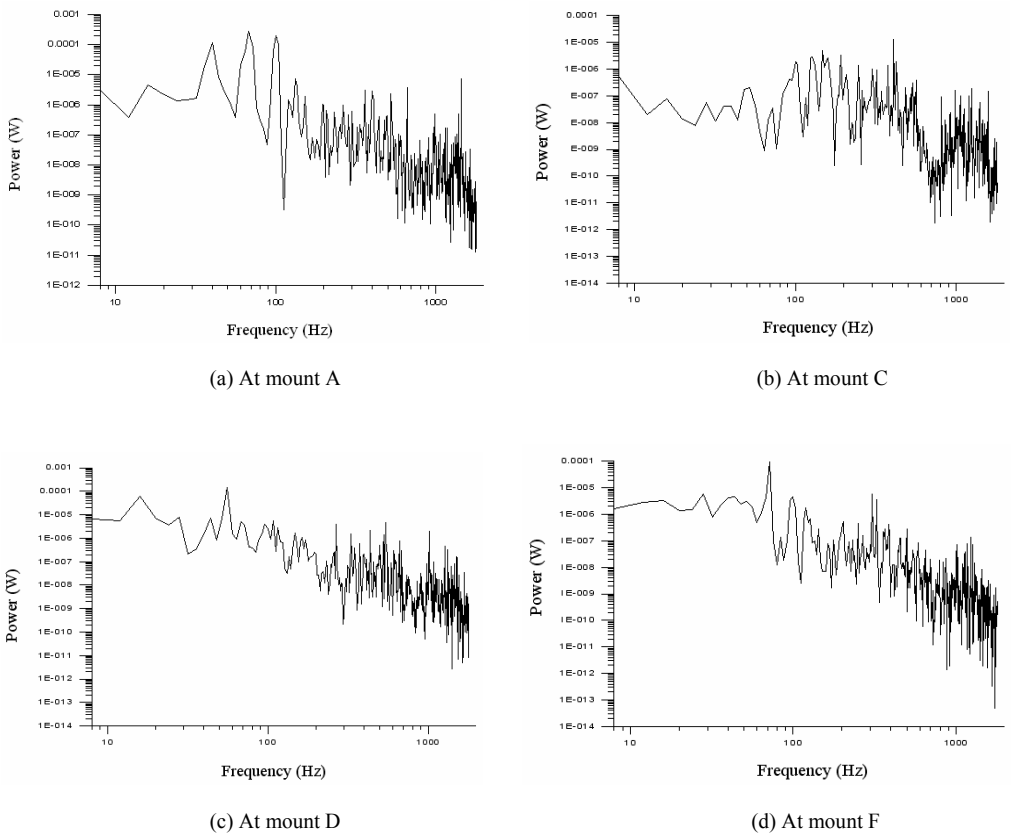

(a) At mount A

(b) At mount C

(c) At mount D

(d) At mount F

Fig. 10. Transmitted power flow spectrum from power unit to the under side of mount A,C,D,F.

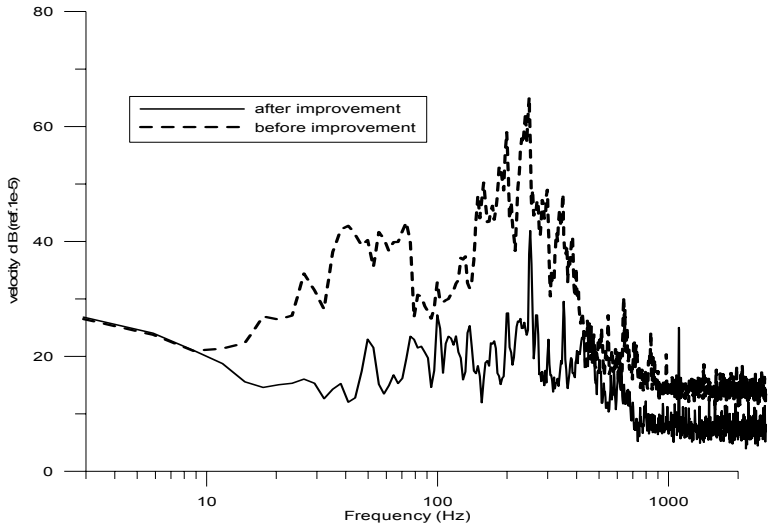

Fig. 11. Measured floor vibration spectra before and after improvement.

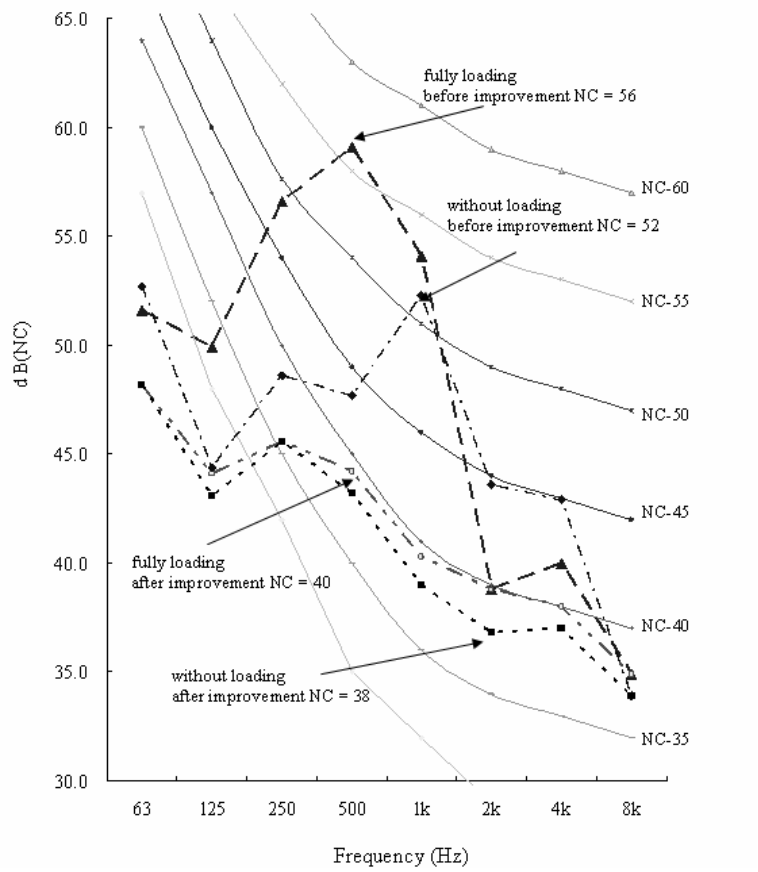

Fig. 12. Measured octave band noise spectra in the accommodation of the 2nd floor above power unit.

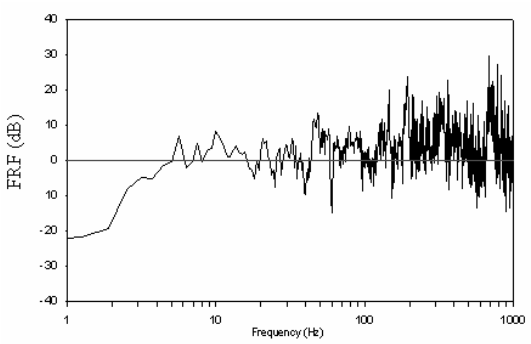

(a) Before improvement

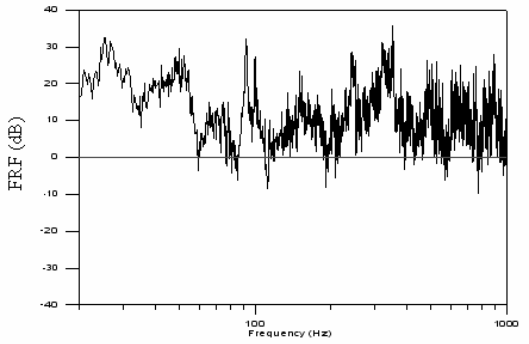

(b) After improvement

Fig. 13. Vibration isolation via mount A.

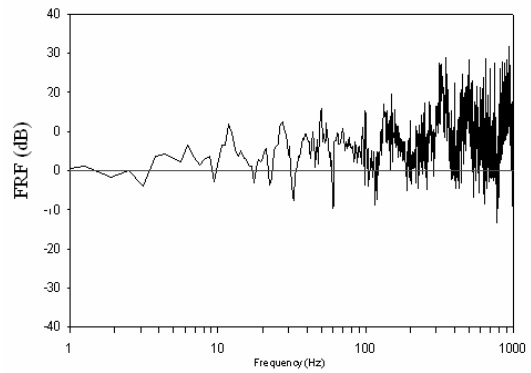

(a) Before improvement

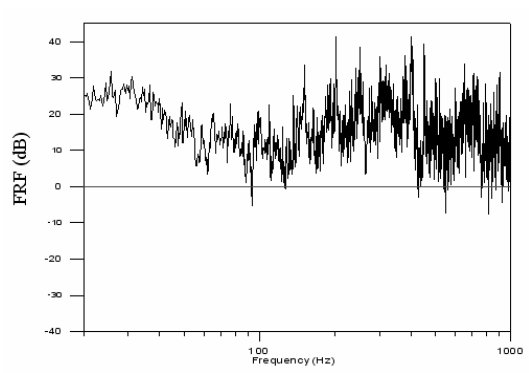

(b) After improvement

Fig. 14. Vibration isolation via mount C.

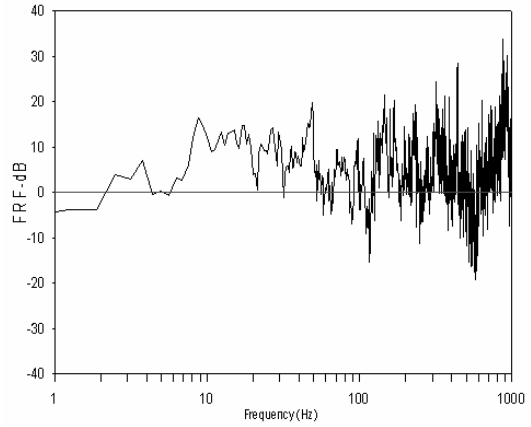

(a) Before improvement

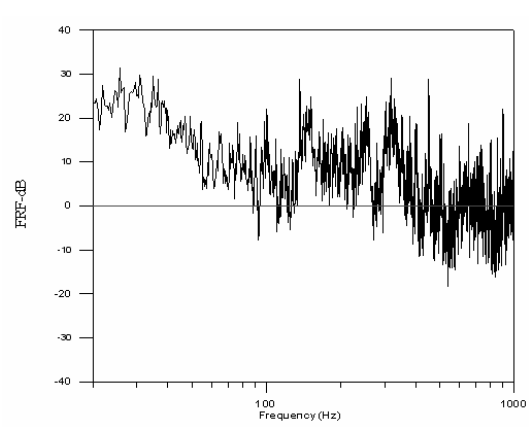

(b) After improvement

Fig. 15. Vibration isolation via mount D.

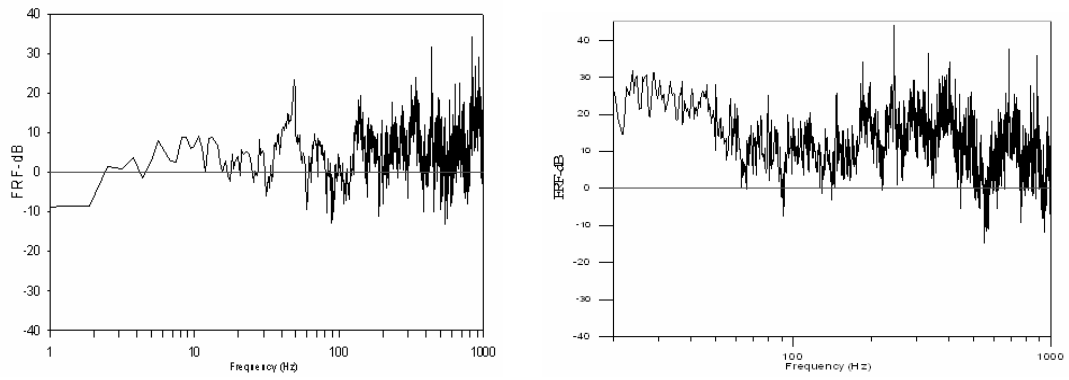

(a) Before improvement (b) After improvement

Fig. 16. Vibration isolation via mount F.

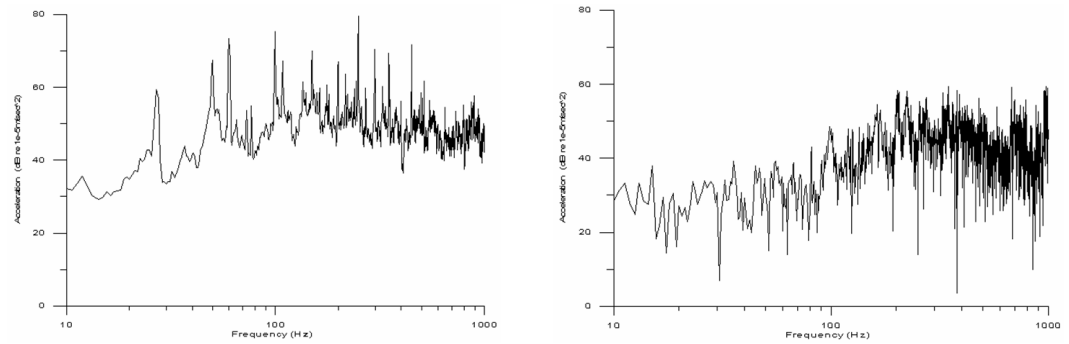

(a) Before improvement (b) After improvement

Fig. 17. Transmitted vibration acceleration spectrum at B during operation of parking tower.

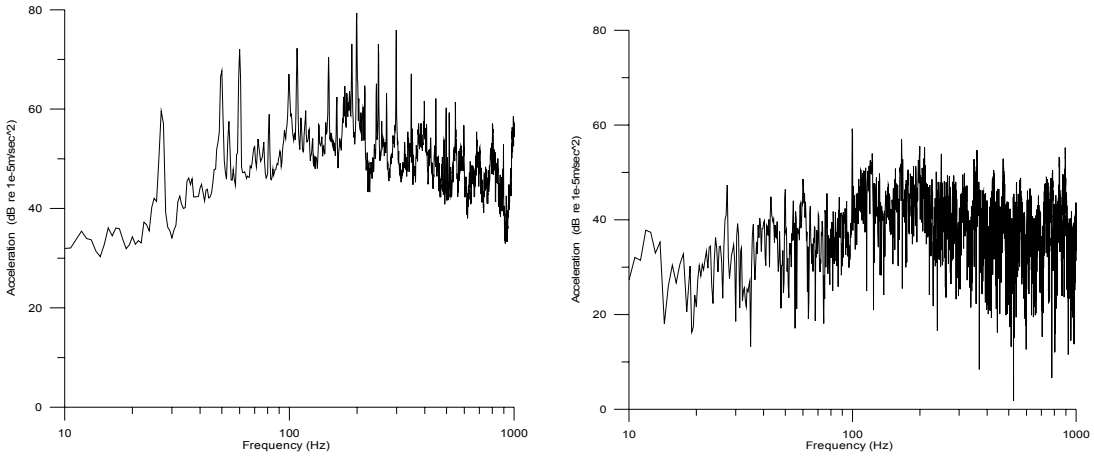

(a) Before improvement (b) After improvement

Fig. 18. Transmitted vibration acceleration spectrum at E during operation of parking tower.

Table 2. Total sound pressure measured right above the parking tower.

Loading conditions	Platform without loading	Platform fully loading	Background
Before Improvement (dB(A))	48.2	52.2	44.3
After Improvement (dB(A))	44.8	45.1	42.4
Noise Reduction Amount (dB(A))	3.4	7.1	

Table 3. NC value measured at the floor right above the parking tower (with expected value less than NC 45).

Loading conditions	Platform without loading	Platform fully loading	Background
Before Improvement (dB NC)	52	56	43
After Improvement (dB NC)	38	40	33
Noise Reduction Amount (dB NC)	14	16	

Table 4. The vibration acceleration at the floor and partition wall in the accommodation right above the parking tower.

Position of vibration measurement	Floor of the second floor			The partition wall in the second floor				
Rank Order	1	2	3	4	1	2	3	4
Dominant frequency (Hz)	670	319	196	292	1174	196	50	100
Vibration acceleration (dB) before improvement	65.9	52.3	51.7	50.3	53.7	51.7	50	46.7
Vibration acceleration (dB) after improvement	22	22.3	29.6	24	26	34	29	26
Vibration reduction Amount (dB)	43.9	30	22.1	26.3	27.7	17.7	21	20.7

Table 5. Vibration isolation value (dB) for the platform under the motor.

Measurement location	Location B		Location E	
Vibration order	1	2	1	2
Vibration wave frequency (Hz)	250	100	200	300
Vibration acceleration before improvement (dB)	80	75	80	76
Vibration acceleration after improvement (dB)	55	39	48	60
Vibration reduction (dB)	25	36	32	16

4. Conclusions

A methodology for the diagnosis and identification of the dominant frequency band for the machine induced vibration power transmission in SC structures has been established in the article. The proposed method can be able to use for the validation of the isolation effectiveness of machine mounts in a broad frequency band. This diagnosis method breaks down the machine induced structure-borne noise and vibration problem into the characterization and ranking of the vibration sources at the generation sites, the power flow analyses in the transmission paths in structures and the noise radiation detection at the receiving points. In applying the developed procedure to the improvement design for the reduction of noise generated by the mechanical parking tower in a SC building, it has attained a substantial attenuation of noise with an amount of 16 dB(NC) in noise criterion index.

Nomenclature

$A_{ijr} = \Phi_{ir}\Phi_{jr}$: Modal constant
c : Sound speed
F_1 : Instantaneous input force
F_2 : Instantaneous output force
G_{ff} : Force spectrum density function
G_{fv} : Cross power spectrum density function

G_{vv} : Vibration velocity spectrum density function
H_{tF} : Frequency response function for force
H_{tv} : Frequency response function for velocity
[M] : Mobility matrix
M_{11} : Driving point mobility at point 1
M_{21} : Transfer mobility at point 2 induced by force acting at point 1
M_{22} : Point mobility at point 2
M_{ij} : Mobility coefficient at d.o.f. i induced by force acting at d.o.f. j
P : Time averaged power
P_{inst} : Instantaneous vibrational power
P_{rad} : Radiation sound power
S : Area of radiation surface
V_1 : Instantaneous input velocity
V_2 : Instantaneous output velocity
V^* : Conjugate of complex velocity V
$\bar{V}^2$: Spatially averaged mean square velocity
[Z] : Impedance matrix
α_{ij} : Four-pole parameters
$[\Phi]$: Mass normalized modal matrix
ω_r : Undamped natural frequency of the r^{th} mode
ω : Exciting frequency
η_r : Structural damping loss factor of the r^{th} mode
φ : Phase angle
ρ : Air density
σ : Radiation efficiency

References

[1] W. Y. Lu and W. H. Wang, Design Method of Structure-Borne Noise Attenuation for Mechanical Parking Tower of a High-rise SC Building, Proceedings of the 15th National Conference on Sound and Vibration, Taipei, (2007).

[2] W. H. Wang and W. Y. Lu, Diagnosis of Muti-Path Structure-Borne Sound Transfer from Resiliently Mounted Machinery in High-Rise Building, Proceedings of the Internoise 2003, Jeju , Seogwipo, Korea,(2003) 3556-3561.

[3] C. M. Mak and Su Jianxin, A study of the effect of floor mobility on structure-borne sound power transmission, Building and Environment, 38 (3) (2003) 443-455.

[4] W. H. Wang, Modelling Machine Induced Noise and Vibration in a Ship Structure, PhD thesis, University of Plymouth,(2000).

[5] Y. P. Xiong, J. T. Xing and W. G. Price, Power Flow Analysis of Complex Coupled System by Progressive Approaches, Journal of Sound and Vibration , 239 (2) (2001) 275-295.

[6] Y. P. Xiong, J. T. Xing and W. G. Price, A general mathematical model of power flow analysis and control for integrated structure-control systems, Journal of Sound and Vibration, 267 (2003) 301-334.

[7] B. A. T. Peterson and B. M. Gibbs, Towards a structure-borne sound source characterization , Applied Acoustics, 61 (2000) 325-343.

[8] P. Gardonio and M. J. Brennan, On the Origins and Development of Mobility and Impedance Methods in Structural Dynamics, Journal of Sound and Vibration, 249 (3) (2002) 557-573.

[9] R. J. Pinnington, Power Transmission from Rigid and Resonant source via Isolator to Resonant and Non-Resonant structure, ISVR Report 114, University of Southampton,(1980).

[10] J. W. Verheij, Transmissin of Structure-Borne Noise, International Course on Systematic Low Noise Desing, SAVOIR, Berlin, (1995) 6.1-6.53.

[11] L. Cremer, M. Heckl and E. E. Ungar, Structure-Borne Sound. Springer-Verlag Berlin, Germany, (1973).

Wei-Yu Lu received his Ph.D. degree from the Department of Systems Engineering and Naval Archi-tecture at the National Taiwan Ocean University.

Wei-Hui Wang is a Professor Emeritus and Director at the Sound and Vibration Research Center, Department of Systems Engineering and Naval Architecture, National Taiwan Ocean University. He received his Ph.D. degree from the Depart-ment of Mechanical and Marine Engineering at the University of Plymouth, UK.